The Astrophysical Journal, 584:316–330, 2003 February 10
© 2003. The American Astronomical Society. All rights reserved. Printed in U.S.A.

HYDROGENATION AND CHARGE STATES OF POLYCYCLIC AROMATIC HYDROCARBONS IN DIFFUSE CLOUDS. II. RESULTS

Valery Le Page, Theodore P. Snow, and Veronica M. Bierbaum
Department of Chemistry and Biochemistry and Center for Astrophysics and Space Astronomy,
University of Colorado, Boulder, CO 80309
Received 2002 June 24; accepted 2002 October 16

ABSTRACT

We have modeled the states of hydrogenation and charge of polycyclic aromatic hydrocarbons (PAHs) in diffuse clouds for molecules ranging from benzene up to species containing 200 carbon atoms. It is found that the hydrogenation state of PAHs strongly depends on the size of the molecule. Small PAHs with fewer than about 15–20 carbon atoms are destroyed in most environments. Intermediate-size PAHs in the range of 20–30 carbon atoms are stripped of most of their peripheral hydrogen atoms, but may be able to survive in the interstellar medium because of the relative stability of their carbon skeleton upon UV photon absorption. Larger PAHs primarily have normal hydrogen coverage (i.e., with each peripheral carbon atom bearing a single hydrogen), with competition between this form and PAHs containing an additional hydrogen. Very large PAHs may be fully hydrogenated, with every peripheral carbon atom bearing two hydrogen atoms. Our finding that extremely dehydrogenated PAH neutrals or positively charged $C_mH_n^{(+)}$, with m ranging from 15 to 30 and $n \leq 2$, can survive in the interstellar medium contrasts with previous work, where it was generally assumed that PAHs losing their hydrogen coverage were quickly destroyed. A mechanism is proposed for the selective growth of these small dehydrogenated PAHs in diffuse clouds with respect to larger PAHs. Finally, our results are compared to previous studies on the hydrogenation and charge states of PAHs.

Subject headings: astrochemistry — ISM: clouds — ISM: molecules

1. INTRODUCTION

Many processes can affect the chemistry and physics of polycyclic aromatic hydrocarbons (PAHs) in the ISM. While there is now a wide acceptance of PAHs as the carriers of the IR emission features at 3.3, 6.2, 7.7, 8.7, and 11.3 μm in protoplanetary nebulae, reflection nebulae, H II regions and in the general interstellar medium (Giard et al. 1994), the ability of PAHs to survive in harsh environments is still largely unknown today. Soon after it was proposed that PAH cations are the carriers of the diffuse interstellar bands (DIBs; Crawford, Tielens, & Allamandola 1985; van der Zwet & Allamandola 1985; Léger & d'Hendecourt 1985), Omont (1986) and Allamandola, Tielens, & Barker (1989) extensively discussed the various processes that govern PAHs in the ISM. Many objections have been raised regarding the viability of PAHs in the ISM (especially in diffuse clouds where the UV field is strong): destruction after absorption of a UV photon, double ionization followed by Coulomb explosion (Leach 1987), dissociative recombination of doubly charged cations (Millar 1992), and destruction involving reactions with O atoms (Duley & Williams 1986).

Attempts to assess these mechanisms have suffered from a lack of experimental work on PAHs. However, there is now a considerable amount of new data on PAHs, and recent progress has been made in measuring the photodissociation of PAH cations by Klippenstein, Faulk, & Dunbar (1993), by the Lifshitz group (Ho, Dunbar, & Lifshitz 1995; Gotkis et al. 1993a, 1993b; Ling, Gotkis, & Lifshitz 1995; Ling, Martin, & Lifshitz 1997; Ling & Lifshitz 1998) and by Leach and coworkers (Rühl, Price, & Leach 1989; Jochims et al. 1993, 1994). Ionization cross sections, as well as UV absorption cross sections, are known for smaller PAHs (Verstraete et al. 1990; Joblin 1992). Electron recombination rates are now known for benzene and naphthalene (Abouelaziz et al. 1993). Finally, chemical reaction rates between PAH cations and neutral molecules (Bohme 1992; Giles, Adams, & Smith 1989; Feng et al. 1996; Snow et al. 1998) or neutral atoms (Snow et al. 1998; Sablier & Rolando 1993; Petrie, Javahery, & Bohme 1992; Scott et al. 1997) have been investigated. The first exploration of the chemistry between a neutral PAH and C^+ has also been accomplished (Canosa et al. 1995), and recent measurements have been carried out on the reactions between aromatic molecules and carbon atoms (Kaiser, Asvany, & Lee 2000).

At the same time, new models of PAH formation have been proposed in circumstellar atmospheres (Frenklach & Feigelson 1989; Allain, Sedlmayr, & Leach 1997). Models have also been built in order to assess the question of ionization and charge state of PAHs in the ISM (Bakes & Tielens 1994; Salama et al. 1996; Dartois & d'Hendecourt 1997) as well as their hydrogenation state (Allain, Leach, & Sedlmayr 1996a, 1996b; Vuong & Foing 2000).

We have developed a comprehensive model for calculating both the state of hydrogenation and the degree of ionization in the diffuse ISM (Le Page, Snow, & Bierbaum 2001, hereafter Paper I). In this paper (Paper II) we use the framework developed in Paper I to assess the hydrogenation and ionization equilibria of PAHs under realistic diffuse cloud conditions. The paper is organized as follows: the model calculations are described in § 2, the results of varying different parameters are described in § 3, the size distribution and physical state of surviving PAHs are analyzed in § 4, and the astrophysical implications and conclusion are summarized in §§ 5 and 6.

2. OVERVIEW OF THE MODEL CALCULATIONS

The physical and chemical properties of PAHs depend strongly on their size. Accordingly, we applied our model to

12 different species spanning a size range from benzene to a hypothetical PAH bearing 200 carbon atoms. The smaller species were chosen from among known compact PAHs, which are thought to be more stable against UV photodissociation (Dartois & d'Hendecourt 1997). The compact PAHs investigated in this study were benzene (C_6H_6), naphthalene ($C_{10}H_8$), anthracene ($C_{14}H_{10}$), pyrene ($C_{16}H_{10}$), coronene ($C_{24}H_{12}$), and ovalene ($C_{32}H_{14}$). Larger PAHs were modeled as graphitic planes with peripheral carbon atoms bearing 1 hydrogen atom each. These large hypothetical PAHs are $C_{50}H_{20}$, $C_{80}H_{24}$, $C_{100}H_{26}$, $C_{120}H_{30}$, $C_{150}H_{40}$, and $C_{200}H_{50}$.

The model was run for each of these species separately. The behavior of the PAHs depends on the processes discussed in Paper I. The most important processes include photoionization, photodissociation, electron recombination, and chemistry involving H and H_2. In these calculations the neutral-neutral chemistry is neglected because it leads to very small changes in the steady-state hydrogenation distribution; for example, assuming a rate coefficient of 10^{-10} cm^3 s^{-1} between radicals and H atoms in the case of the $C_{30}H_n^{(+)}$ model calculation leads to a small change in the distribution (only a few percent of the PAHs are distributed differently).

The model gives the equilibrium distribution of the PAH under investigation; i.e., the way in which the species is distributed over its various hydrogenation and charge states. For example, a light species such as pyrene will be almost completely dehydrogenated in most environments, because of the low number of degrees of freedom available to store the energy subsequent to UV absorption. In contrast, a large species such as $C_{200}H_{50}$ can be completely hydrogenated (i.e., $C_{200}H_{100}$, with each of the 50 peripheral carbon atoms bearing 2 hydrogen atoms).

The results depend strongly on the assumed diffuse cloud physical conditions. The conditions are set by specifying the environmental parameters n_t, the total H density ($n_t = n_H + 2n_{H_2}$); f, the ratio of molecular hydrogen to atomic hydrogen densities ($f = n_{H_2}/n_H$); χ the scaling factor of the UV field ($\chi = 1$ for the normal interstellar field); T, the kinetic temperature; and n_e/n_t the specific ratio of electron density to total H density.

For a standard diffuse cloud we set $n_t = 100$ cm^{-3}, $f = 0.5$ (i.e., $n_H \sim 50$ cm^{-3} and $n_{H_2} \sim 25$ cm^{-3}), $\chi = 1$, $T = 100$ K, and $n_e/n_t = 1.4 \times 10^{-4}$. The electron density n_e is set equal to the number density of carbon ions, based on the assumption that carbon is completely ionized and the gas is otherwise neutral. Our adopted carbon abundance in the gas is $1.4 \times 10^{-4} n_t$ (Sofia et al. 1997). We then examined the effects of varying these input parameters.

3. MODEL RESULTS: ISOLATION OF PARAMETERS

3.1. *Hydrogenation Equilibrium*

The hydrogen molecular fraction f was kept constant ($f = 0.5$), and χ, T, and n_e/n_t were given their standard values as well, while the total density n_t was varied. The results are presented in Figure 1. Two different behaviors can be seen in this figure. First, the proportion of hydrogenated states increases when the hydrogen density increases, which is a simple consequence of the increased number of collisions between the PAH cation and H atoms. Second, the proportion of neutrals increases with hydrogen density because we choose to keep the n_e/n_t ratio constant, and thus increasing the hydrogen density leads to an increase of the electron density. In Figure 1*b* it can be seen that for a very high hydrogen density the coronene PAH approaches its normal hydrogenation state, which is 12. In Figure 1*c*, for hydrogen density about 100 cm^{-3} the ovalene PAH is expected to be primarily divided into three different hydrogenation states, which are $C_{32}H_{13}^{(+)}$, $C_{32}H_{14}^{(+)}$, and $C_{32}H_{15}^{(+)}$, the major contribution coming from $C_{32}H_{14}^{+}$. For larger PAHs like $C_{50}H_{20}$ (Fig. 1*d*) the equilibrium distribution is peaked at the normal hydrogenation state irrespective of the hydrogen density. When n_t increases, the protonated form $C_{50}H_{21}^{+}$ begins to compete with the normal $C_{50}H_{20}^{(+)}$ form, a trend that is even more pronounced for larger PAHs.

3.1.1. *Dependence on the Hydrogen Density*

The most striking aspect of our model results is the extreme sensitivity of the hydrogenation state of PAH cations to the total hydrogen density. There is a competition between the UV processes, which tend to dehydrogenate the PAH cations, and the reactivity between the PAH cations and H atoms, which tends to repopulate the more hydrogenated states. In most cases one or the other dominates, and we predict either an overwhelming preponderance of extremely dehydrogenated species or a concentration of PAH cations with nearly normal hydrogenation (where each peripheral carbon atom is bonded to 1 hydrogen atom). It is only when the competing effects of the UV field intensity and the hydrogen density are closely balanced that we see a range of partially hydrogenated species (in Fig. 1*b* see $C_{24}H_n$ with n between 4 and 12 and with $n_t = 100$ cm^{-3}, for example).

For large PAH cations the normal hydrogenation state is favored, because photodissociation ceases as the PAHs become large and have sufficient internal degrees of freedom to withstand absorption of UV photons (this is discussed in detail below). For PAHs with 50 or more carbon atoms, there are no dehydrogenated or intermediate species, and the PAH becomes entirely concentrated in forms having normal hydrogenation or normal-plus-one hydrogen coverage (i.e., $C_{50}H_{20}$ and $C_{50}H_{21}$, for example). This occurs because the radiative association rate decreases when the PAHH state is reached, but is high for all levels of hydrogenation up to the normal PAH state. (PAHH represents PAH containing more hydrogen than in the normal state.) That is, for large PAH cations the addition of hydrogen atoms is facile (and loss is difficult) until the PAHH level of hydrogenation is reached. Therefore, provided that the UV field is not too strong, the large PAH cations will migrate toward a mixture of the normal state (e.g., $C_{50}H_{20}^{+}$) and the next higher hydrogenation state ($C_{50}H_{21}^{+}$).

This behavior reflects the high rates for association of dehydrogenated PAH cations in reactions with H or H_2; these rates have been measured for dehydrogenated PAH^+ (Le Page et al. 1999a, 1999b) as well as for extremely dehydrogenated hydrocarbons (Scott et al. 1997). These model results also reflect the low reactivity of $PAHH^+$ and more fully hydrogenated $PAHH_n^+$ with H and H_2. For example, while the protonated pyrene $C_{16}H_{11}^{+}$ adds up to 6 hydrogen atoms in consecutive steps (Le Page, Snow, & Bierbaum, unpublished results) the rate of association at each step was found to be about 50 times smaller than in the case of normal PAH^+.

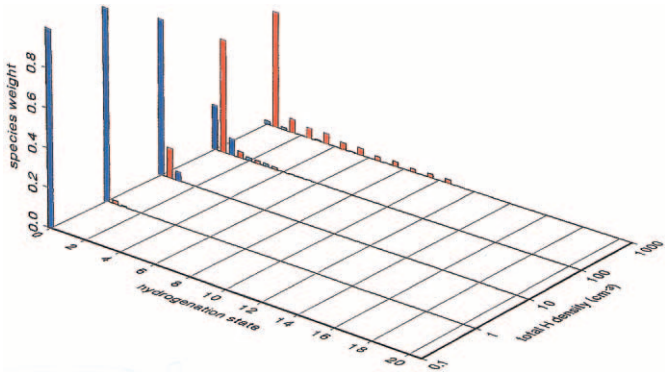

FIG. 1*a*

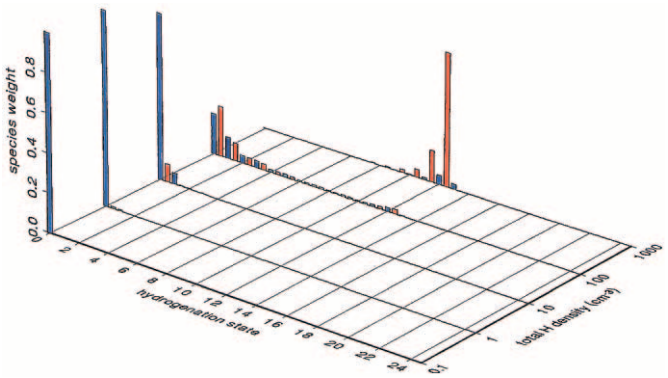

FIG. 1*b*

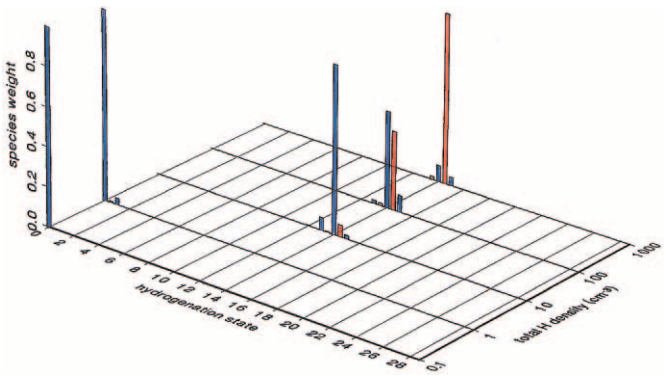

FIG. 1*c*

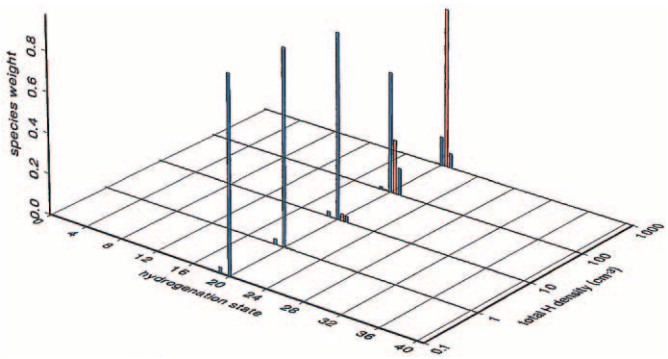

FIG. 1*d*

FIG. 1.—Variation of the charge and hydrogenation state distributions for four different PAHs: (*a*) $C_{16}H_n$, (*b*) $C_{24}H_n$, (*c*) $C_{32}H_n$, and (*d*) $C_{50}H_n$ as a function of total hydrogen density. Blue bars represent cations and red bars represent neutrals. The first bar on the left side of panel *a* represents the C_{16} cation; this is the only form that can survive when the local hydrogen density is as low as 0.1 cm^{-3}. Other states arise when the hydrogen density is higher; for example, when $n_t = 100$ cm^{-3} it is possible to detect several different hydrogenation and charge states. In this figure the states are sorted first by charge, and then according to the hydrogen coverage; thus, for $n_t = 100$ cm^{-3} the first bar at the left represents the C_{16} cation, then the second (major) bar represents the C_{16} neutral, the third one the $C_{16}H$ cation, the fourth the $C_{16}H$ neutral, and so on.

It is thus expected that a PAH cation will be either in an extremely dehydrogenated state or in its normal state, depending on the ratio between the hydrogenation rate and the hydrogen loss rate due to photodissociation. The existence of partially hydrogenated species in the ISM appears to be a transient phenomenon, with a consequently low probability of occurrence. According to our model, only PAH cations with a few peripheral hydrogens or, inversely, with nearly normal hydrogen coverage, can be significant constituents of diffuse clouds.

3.1.2. *The Probability of Carbon Loss*

It is generally assumed that only PAH cations with their normal hydrogen content have interstellar relevance, and that when PAHs lose these peripheral atoms they are quickly destroyed. However, this assumption is not supported by consideration of the energetics of the carbon-carbon bonds. While it is true that a PAH^+ with fewer hydrogen atoms will be less stable when absorbing a UV photon because of its reduced number of degrees of freedom, this does not ensure that the PAH^+ will be completely destroyed. Indeed, this will be true if the carbon skeleton, stripped of most of its hydrogen atoms, is then easily photodissociated. However, losing an H atom requires only one bond to be broken, requiring less than about 5 eV; in contrast, the ejection of 1 or 2 carbon atoms in a compact PAH^+ requires at least 2 bonds to be broken, with a total required energy of about 8 eV.

As an estimate of the energy needed to eject a C atom or a C_2 or C_3 fragment, one can examine the corresponding quantities for graphite. These quantities have been estimated by Léger et al. (1989) for use in their elegant theory of photo-thermo-dissociation of PAHs exposed to a UV field. They found that a C, C_2, and C_3 ejection will require, respectively, 7.4, 8.5, and 8.0 eV. A dissociation process that requires about 8 eV in energy will occur with a rate considerably lower than a normal H loss process, which requires less than 5 eV. Therefore, it is possible to dehydrogenate a PAH while leaving the carbon skeleton intact. These PAHs will survive in an extremely dehydrogenated form, with possibly only a few H atoms attached. Therefore, in our model we assume that there is no carbon loss within the timescale of the hydrogenation gain/loss processes, and we then determine the distribution of hydrogenation states in the steady-state limit.

In order to test this assumption we have calculated the time needed to achieve the steady-state distribution. The migration time for a PAH, which depends on the local environmental parameters, is defined as the time elapsed during the process that transforms the initial PAH distribution within a given carbon skeleton into the steady-state distribution. This migration time strongly depends on the initial PAH distribution, and consequently we have carried out two different calculations: in the first it is assumed that the

TABLE 1
MIGRATION TIMES (IN yr) CALCULATED FOR FIVE DIFFERENT PAHs AND FIVE DIFFERENT TOTAL HYDROGEN DENSITIES

SPECIES	HYDROGENATION	TOTAL HYDROGEN DENSITY (cm^{-3})				
		0.1	1	10	100	1000
C_{16}	Dehydrogenated	*	*	1.4	4.2	5.7
	Hydrogenated	53	54	57	110	150
C_{24}	Dehydrogenated	*	*	*	35	230
	Hydrogenated	120	120	130	750	4.4
C_{32}	Dehydrogenated	*	*	42,000	250	110
	Hydrogenated	7300	27,000	*	2.0	*
C_{50}	Dehydrogenated	200,000	18,000	2000	260	95
	Hydrogenated	*	*	*	1.1	*
C_{200}	Dehydrogenated	64,000	49,000	5900	690	92
	Hydrogenated	2600	260	26	2.4	*

NOTE.—These migration times correspond to the distribution displayed in Fig. 1 for pyrene, coronene, ovalene and C_{50}, and of Fig. 8*a* for $C_{200}H_{50}$. They are defined as the time that is needed for a species to reach a distribution of charge and hydrogenation states which is close to the stable one obtained at the "infinite time" limit (steady-state limit) as displayed on Figs. 1 and 8*a* (see last section of Paper I). These migration times strongly depend on the initial distribution of the PAH at "zero" time. In this table "dehydrogenated" designates that the initial distribution is chosen as a carbon skeleton without hydrogen atoms, while "hydrogenated" indicates a PAH bearing a normal hydrogen coverage (e.g., $C_{32}H_{14}$ for ovalene). Asterisks indicate migration times shorter than 1 yr. See text in § 3.1.2 for details.

PAH is initially concentrated in its completely dehydrogenated form (e.g., C_{24} for coronene), and in the second it is assumed that the initial PAH is in its normally hydrogenated form (e.g., $C_{24}H_{12}$ for coronene). The results presented in Table 1 show that equilibrium is reached within a few tens of years at most, provided that the initial distribution of the PAH (dehydrogenated or normally hydrogenated) is the one that is expected to dominate in this particular size range. It is possible for this to occur if we assume that the processes that transform one PAH (e.g., $C_{24}H_n^{(+)}$, neutral or cation) into another PAH family (e.g., $C_{22}H_m^{(+)}$) are mainly carbon loss after photon absorption or carbon insertion through reaction between C^+ and neutral PAH. Thus, as the PAH families are of similar size—they differ only by several carbon atoms—it is highly probable that the steady-state distribution of the first family, which determines the initial distribution of the second family, will be of the same type (i.e., extremely dehydrogenated or normally hydrogenated). The two exceptions to this generic behavior are the processes of PAH coalescence (e.g., $C_{24}^+ + C_{24} \rightarrow C_{48}^+$) as well as the few reactions in which the initial and final PAH family have a very different hydrogen coverage at the steady-state limit. The latter corresponds, for example, to the case $C_{32}H_{14}^+ + h\nu \rightarrow C_{30}H_{12}^+ + C_2H_2$ in an environment where $n_t = 10\ cm^{-3}$ (see Fig. 1*c*). In such an environment the $C_{30}H_{12}^+$ species will be converted to the dehydrogenated $C_{30}^{(+)}$ species because the $C_{30}H_{12}^+$ species does not have enough degrees of freedom to retain its hydrogen coverage in the normal UV field. For these special and somewhat unusual cases in which the initial and final hydrogen coverage are very different, the migration times can be much longer and the hydrogenation equilibrium might not be reached before another carbon loss could occur (e.g., $C_{30}H_{12}^+ + h\nu \rightarrow C_{28}H_{10}^+ + C_2H_2$). This behavior comes from the fact that in our model, and for a given environment, there must be a limit at which the hydrogen addition rate is almost equal to the photodissociation rate, thus drastically increasing migration times. This case is exemplified in Figure 3*b*, where the C_{24} family is split into two distributions at low *f* values, which is an indication that hydrogenation and photodissociation processes are effectively competing. However, apart from these unusual cases, Table 1 shows that the hydrogenation equilibrium is generally reached within a time shorter than a few tens of years. The assumption that this equilibrium is achieved before any other minor processes can occur is thus valid in most cases.

The "chemical" stability of extremely dehydrogenated PAHs has not been investigated for reactions involving species other than C^+ or H and H_2; it is thus possible that these reactive species will disappear quickly by reacting with other abundant species of the diffuse ISM such as O, N, or OH. However, we have found in our experimental study of benzene, naphthalene, and pyrene that most reactions involving PAH^+ are addition reactions, especially for larger PAH^+. For example, for reactions between N atoms and PAH^+we found that the branching ratio for addition was increasing from about 10^{-3} ($C_6H_6^+ + N \rightarrow C_6H_6N^+$) to 0.7 ($C_{10}H_8^+ + N \rightarrow C_{10}H_8N^+$) and greater than 95% ($C_{16}H_{10}^+ + N \rightarrow C_{16}H_{10}N^+$). In our study the addition reactions proceed through termolecular stabilization, but it is expected that for large PAHs radiative association will be efficient as well. If this is the case, the extremely dehydrogenated PAH may be chemically stable because the bond energy between the two fragments (the PAH and, for example, N) will not be large enough to make the complex photostable in the standard interstellar radiation field (ISRF). We can expect this bond energy to be about 5 eV or less, which makes this bond the weakest of the complex and thus the most prone to destruction. If this picture is valid, then the lifetime of extremely dehydrogenated PAHs will be controlled by condensation reactions such as, for example, $C_{24}^+ + C_{24} \rightarrow C_{48}^+$.

3.1.3. *Dependence on Other Parameters*

Our assumption that no other processes compete with dehydrogenation is probably not valid for the smaller

PAH^+ species such as benzene or naphthalene, for which the C_n loss rate is likely to be as fast as the hydrogen loss rate. However, for PAH cations such as pyrene or larger, the C_n loss rate is expected to be much lower than the H loss rates.

Other parameters play an important role in the hydrogenation state of PAHs, especially the UV field intensity, which is represented by χ in the model. Figures 2 and 3 show the dependence of the hydrogenation states of four PAHs on χ, as well as the dependence on the H_2 fraction (f) in the cloud. It is obvious that an increase in χ will have exactly the opposite effect as an increase in the hydrogen density. For example, decreasing the UV field strength by an order of magnitude will have the same consequence as increasing the hydrogen density by an order of magnitude. This arises in our model because for each process that is proportional to χ (dissociation with H or H_2 losses and ionization), there is an opposing process that is directly proportional to the local hydrogen density (radiative addition of H atoms and electron recombination).

In Figures 1, 2, and 3 we show results for which only one parameter ($n_t, \chi,$ or f) is varied while the others are kept constant $n_t = 100$ cm^{-3}, $\chi = 1$, $f = 0.5$, $T = 100$ K, and $n_e/n_t = 1.4 \times 10^{-4}$). This approach, in which all parameters are uncoupled from each other, allows us to clearly discriminate between the influences associated with each parameter. Thus, the variation of the PAH hydrogenation state distribution for $C_{32}H_n$ between $n_t = 10$ cm^{-3} and $n_t = 100$ cm^{-3}, for example, with the other parameters having their standard values, is not to be considered as representative of a real case, where $n_t = 10$ cm^{-3} would represent the hypothetical outer edge of a cloud and $n_t = 100$ cm^{-3} might represent the inner core of the same cloud. A more realistic model would require that the other important parameters χ, f, T, and n_e are varied in accordance with the physical laws governing the environment (e.g., van Dishoeck & Black 1986). Some of our assumptions are better than others. For example, maintaining a constant value for n_e/n_t throughout the entire cloud is probably sound, since it is based on a constant C/H ratio and the assumption that carbon is fully ionized throughout a diffuse cloud, which is realistic even for relatively dense diffuse clouds. In contrast, we can expect that f and T will vary considerably throughout a cloud. The influence of varying f can be drastic, as is shown by the

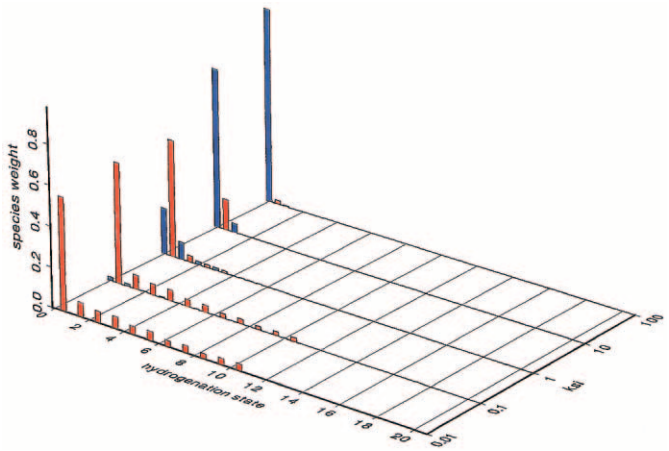

FIG. 2*a*

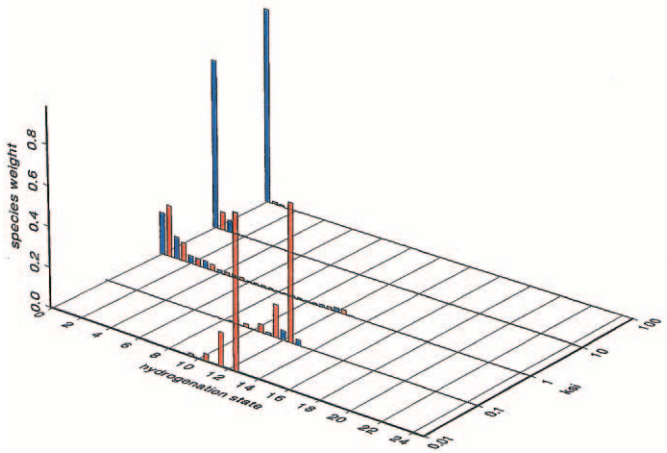

FIG. 2*b*

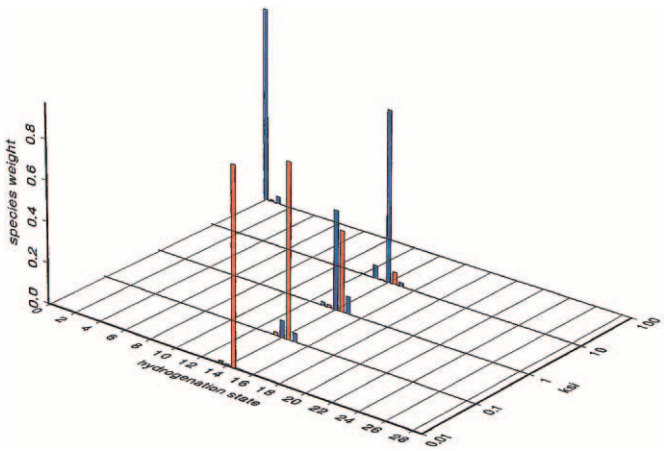

FIG. 2*c*

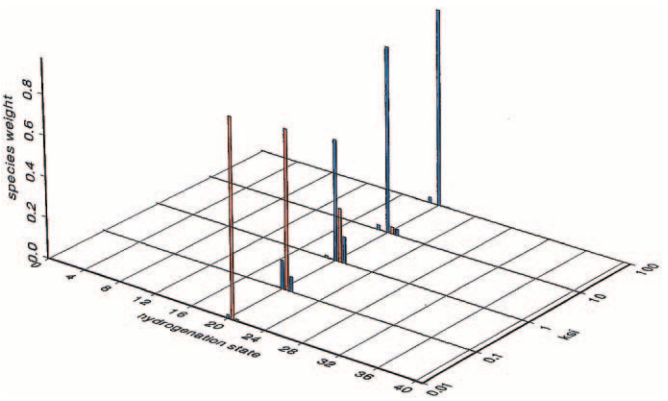

FIG. 2*d*

FIG. 2.—Variation of the charge and hydrogenation state distributions for four different PAHs (pyrene, coronene, ovalene, and $C_{50}H_{20}$) when varying the intensity of the UV field through the χ factor. Blue bars represent cations and red bars represent neutrals. When a PAH is immersed in a weak UV field the association of H to the carbon skeleton is more effective because of a reduced photodissociation rate. However, for the small PAH family $C_{16}H_n$, the photodissociation rate remains important and the PAH is mostly dehydrogenated, even in a UV field that is only 1/100 of the standard field. The χ factor for which the PAH is able to add hydrogen atoms increases with increasing size of the PAH and for $C_{50}H_{20}$ (panel *d*) the PAH can remain close to its normal hydrogenation state even in a UV field that is 100 times higher than the standard interstellar UV field.

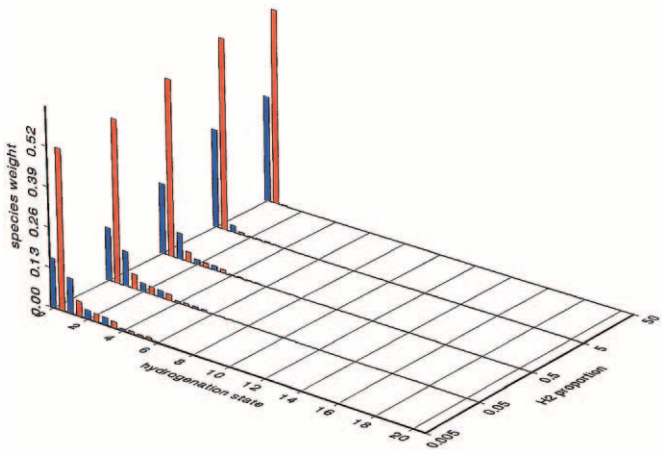

FIG. 3*a*

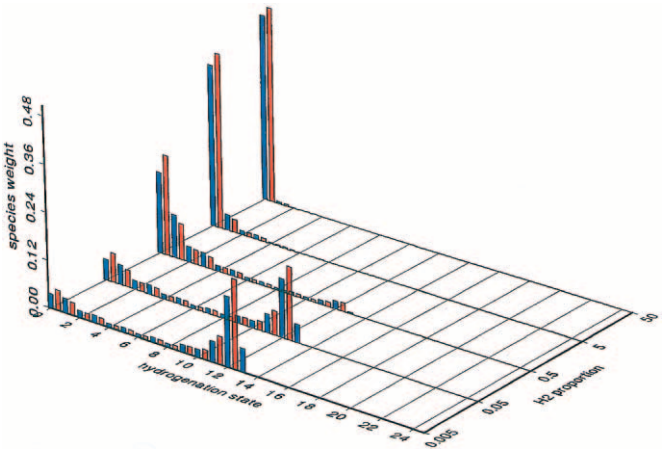

FIG. 3*b*

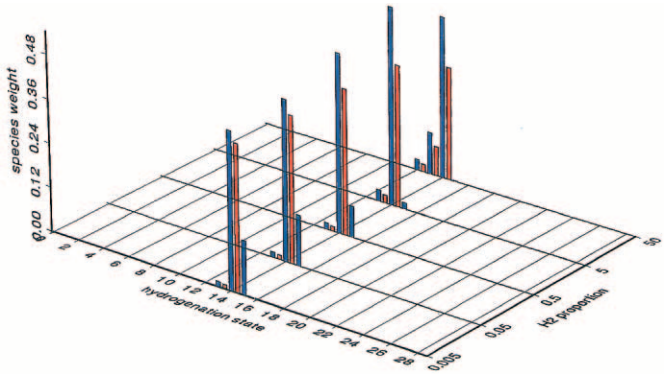

FIG. 3*c*

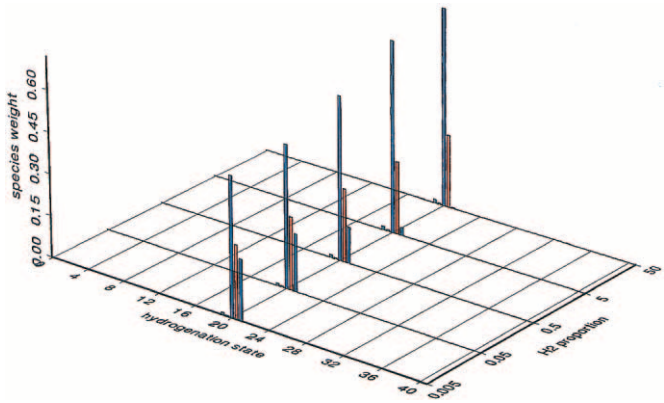

FIG. 3*d*

FIG. 3.—Variation of the PAH hydrogen and charge states distribution when varying the proportion of H_2. Blue bars represent cations and red bars represent neutrals. For a very low proportion of H_2 in the case of coronene (panel *b*) a noticeable proportion of the PAH is able to survive with its normal hydrogen coverage. When the H_2 proportion increases the PAH is mostly dehydrogenated because H_2 is generally less effective than H in the hydrogenation process. For larger PAHs like $C_{50}H_{20}$ (panel *d*) this trend almost disappears; larger PAHs are much less sensitive to the local environment.

example of coronene (Fig. 3*b*), where we see that an increase of the H_2 fraction will appreciably lower the hydrogenation rate because H_2 is less efficient than H atom in the hydrogenation process.

To elaborate further on the effect of varying f, we note that H_2 inhibits hydrogenation mainly because this molecule converts two reactive H atoms into a single less reactive species. Another important trend that can be seen in Figure 2 is the role of χ with respect to the efficiency of the hydrogenation of PAH^+. This figure shows that a small value of χ will not lead to more hydrogenation because, even if a mild UV field increases hydrogenation, it will also lead to a decrease of the cations, which are the only species reacting with H in our model. In the same way, a large value of χ leads to a decrease of hydrogenation (see $\chi = 100$ in Fig. 2*c*, for example). The maximum hydrogenation occurs at $\chi \sim 1$, where there is a balance between a large cation population and a moderate loss of H due to an increase of the UV intensity.

The influence of the two other parameters, T and n_e/n_t, is far less critical, at least under the assumption made in Paper I that the rate coefficients for radiative association with H and H_2 are temperature-independent. In our model the only temperature-dependent parameter is the rate of recombination with electrons, which is assumed to have a $T^{-1/2}$ dependence (Bates 1988). This effect is not important in the temperature range under investigation ($T < 400$ K) and can be neglected. The variation of n_e/n_t within an acceptable range (from 10^{-4} to 5×10^{-4}) also leads to small changes in the ratio of cations to neutrals, and thus will not be discussed further.

In summary, from the model results on the hydrogenation states of pyrene, coronene, ovalene, and $C_{50}H_{20}$ as functions of the local hydrogen density in typical diffuse clouds, it is clear that the transition between an extremely dehydrogenated PAH and a normally hydrogenated PAH occurs for PAHs between coronene (24 C) and ovalene (32 C). We thus conclude that, depending on the local environmental parameters, PAHs will remain in their normal hydrogenation state (e.g., $C_{32}H_n^+$ with $n \approx 14$) if they contain more than 25–30 carbon atoms.

3.1.4. *Photodissociation of PAHs*

Many authors have suggested that PAHs in the ISM could be either partially dehydrogenated (Du, Salama, & Loew 1993) or even beyond the normal level of hydrogenation (Du et al. 1993; Schutte, Tielens, & Allamandola 1993;

Bernstein, Sandford, & Allamandola 1996; Pauzat et al. 2001), depending on the local environment. However, there are few quantitative studies in the literature that assess this fundamental question.

As noted above, the hydrogenation state of PAHs primarily depends on two rate coefficients: first, the hydrogenation rate, which is a function of the hydrogen density (both atomic and molecular) and the cation fraction; and second, the photodissociation rate, which is a strong function of both the PAH size and the UV field intensity. The resulting hydrogenation equilibrium is the balance between the photodissociation rate due to absorption of UV photons (which tends to decrease the hydrogen coverage through hydrogen loss) and the hydrogenation rate (which opposes this process through radiative addition of hydrogen). Many workers have studied this equilibrium in order to estimate the minimum PAH size that can withstand the UV field, and it is sometimes assumed that only PAHs that are able to retain their peripheral hydrogen atoms can survive in the ISM. The study of such equilibrium requires estimates of both the rate of photodissociation and the rate of hydrogenation.

Usually, a statistical theory is used for evaluating the photodissociation process, while the hydrogenation rate is assumed to proceed at the collision rate (the Langevin rate, which is about 10^{-9} cm^3 s^{-1}) in reactions between cations and H atoms. Sometimes the contribution of neutrals through radical-radical reactions is taken into account (Allain et al. 1996b).

Different statistical theories of unimolecular reactions have been used to estimate the photodissociation rate. For example, Omont (1986) has employed the general theory of unimolecular reactions (Benson 1976) and has assigned a minimum size for PAH survival of about 30 carbon atoms. Allamandola et al. (1989), using the QRRK theory of Barker (1983) reached the same conclusion and have deduced a minimum size for PAHs to be stable against H loss of about 25–30 carbon atoms. Léger et al. (1989), using their photo-thermo-dissociation theory, have estimated the carbon skeleton to be stable even for PAHs with about 15 carbon atoms after absorption of a single 10 eV photon.

Finally, Allain et al. (1996a, 1996b), using the RRK theory developed by Jochims et al. (1994), concluded that PAHs with fewer than 50 carbon atoms are destroyed in the ISM because the photodissociation rate with ejection of an acetylene molecule (C_2H_2) is larger than the association rate between C^+ and a neutral PAH for molecules containing fewer than 50 carbon atoms. It is important to note that the results of Léger et al. and Allain et al. are not contradictory and should not be compared, because the former deals with loss of a C_n fragment (C, C_2, or C_3) from the PAH skeleton, which is a process requiring about 8 eV, while the latter is a study of C_2H_2 loss, which is a process having an endothermicity of about 5 eV and is thus much more likely to remain important for larger hydrogenated PAHs.

We note also that the predictions of Allamandola et al. are in very good agreement with our own calculations (see Paper I), where we found that for a normal UV field and a hydrogen density in the 10–100 cm^{-3} range, the minimum size for a PAH at which hydrogenation starts to compete with photodissociation is about 25 carbon atoms. This result comes from the fact that the QRRK theory used by Allamandola et al. and our RRKM calculations follow the same kind of law for large PAHs, and thus the discrepancy between these two sets of calculations is not expected to be large.

3.2. *The Charge State of PAHs in the Diffuse ISM*

3.2.1. *The Basic Processes*

The charge state of PAHs in diffuse clouds mainly depends on four rate coefficients: (1) the ionization rate $k_{\rm ion}$; (2) the recombination rate $k_{\rm rec}$; (3) the electron attachment rate k_e; and (4) the photodetachment rate $k_{\rm ph}$, all of which are a priori dependent on the size of the PAH. These rates are associated with the following processes:

$$\mathrm{PAH} + h\nu \xrightarrow{k_{\rm ion}} \mathrm{PAH}^+ + e$$

$$\mathrm{PAH}^+ + e \xrightarrow{k_{\rm rec}} \text{products}$$

$$\mathrm{PAH} + e \xrightarrow{k_e} \mathrm{PAH}^-$$

$$\mathrm{PAH}^- + h\nu \xrightarrow{k_{\rm ph}} \mathrm{PAH} + e\ .$$

The rates for these processes have been estimated in Paper I. We present here results (Fig. 4) on the charge distribution of PAHs of selected sizes (pyrene, coronene, C_{50}, and C_{100}) at three different hydrogen densities. From Figure 4 it is clear that the anion proportion is usually low in diffuse clouds, and thus the neglect of anion chemistry is a reasonable assumption; however, anions may dominate in denser environments, such as molecular clouds (e.g., Lepp & Dalgarno 1988).

3.2.2. *Comparison with Previous Studies of PAH Ionization Equilibrium*

Although there have been only two previous models of hydrogenation equilibrium (Allain et al. 1996b; Vuong & Foing 2000) of PAHs, there have been more calculations of ionization equilibrium, allowing us to make comparisons. Several workers have investigated the PAH charge state in the ISM, and the results depend on the method for estimating the four rates involved. The rates are difficult to estimate, since there are few experimental data, which necessitates the use of theoretical values; in addition, the experimental data that do exist are limited to small PAHs. The extrapolation of these results to very large PAHs is not straightforward.

There are two radically different approaches available when trying to estimate values for unmeasured parameters involved in the calculation of the charge state balance for large PAHs. The PAHs can be treated as free molecules and their properties extrapolated from smaller PAHs (benzene, naphthalene, pyrene, coronene, etc.); alternatively, the large PAHs can be treated as small grains by using a bulk solid approach.

General examples of the solid-state treatment of small grains can be found in Spitzer (1978) and Draine & Sutin (1987). This approach has been applied specifically to large PAHs by Bakes & Tielens (1994), Salama et al. (1996), Snow et al. (1995), and Dartois & d'Hendecourt (1997).

The alternate approach, in which the PAH is considered as a free molecule and thus expected to have physical properties that can be deduced from smaller PAHs, is exemplified by the analysis of Allain et al. (1996a). In this study, most of the properties of large PAHs were extrapolated

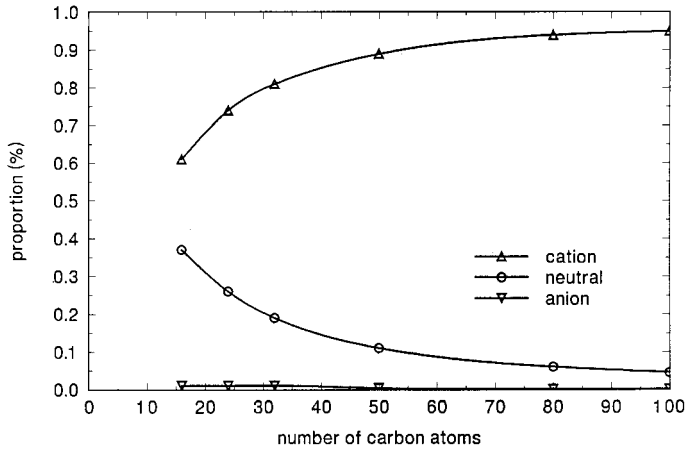

FIG. 4*a*

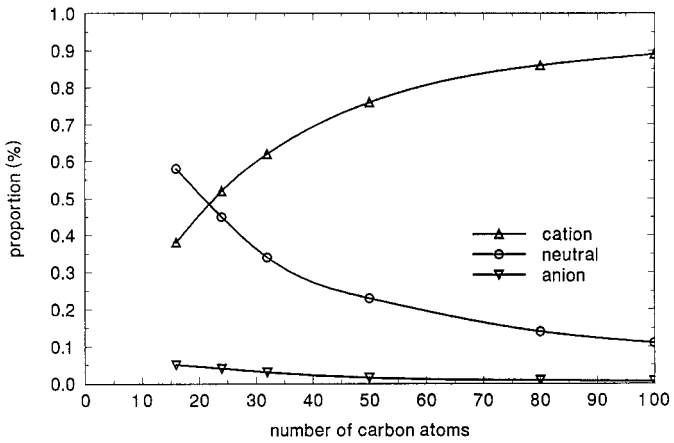

FIG. 4*b*

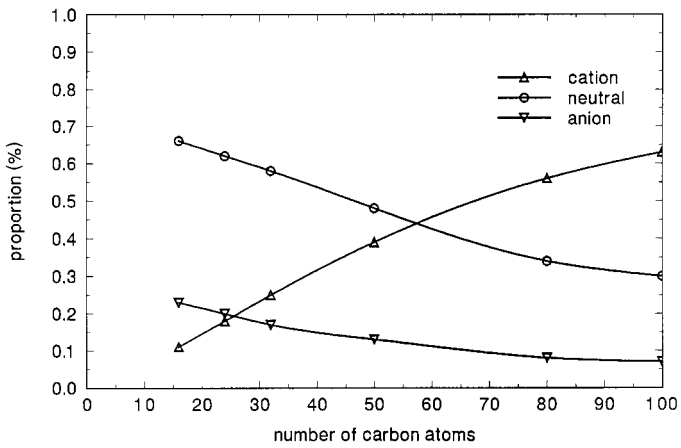

FIG. 4*c*

FIG. 4.—Distribution of PAHs over the cationic, neutral and anionic charge states for three different hydrogen densities of (*a*) 10 cm^{-3}, (*b*) 25 cm^{-3}, and (*c*) 100 cm^{-3}.

from experimental work carried out on smaller PAHs having sizes up to coronene.

We have compared our rate coefficient calculations to both the solid-state and free-molecule results of previous work, adopting Salama et al. (1996) to represent the former and the analysis of Allain et al. (1996a) the latter. These two studies rank among the more extensive analyses of PAHs in the ISM. The comparisons are shown in Table 2. Although the anion contribution was not included in the work of Allain et al., we include their results in the table because their calculation of the ionization rate of PAH is probably the most detailed carried out to date.

3.2.3. *The Effect of Individual Parameters*

Photoabsorption cross section.—In our calculations we have used an average UV absorption cross section from the work of Joblin (1992), measured in a mixture of neutral PAHs, instead of using a different cross section for each PAH, as was done by Allain et al. (1996a). The differences between our results and the more detailed values of Allain et al. are not drastic, as our rates of photoionization are within a factor of 2 of their values. The calculations of Salama et al. (1996) also compare well with the results of Allain et al., although Salama et al. did not use the interstellar field of

TABLE 2

COMPARISON OF OUR CALCULATED IONIZATION, ELECTRON RECOMBINATION, ELECTRON ATTACHMENT, AND PHOTODETACHMENT RATES (IN s^{-1}) WITH THE RATES ESTIMATED BY SALAMA ET AL. (1996) AND ALLAIN ET AL. (1996a, 1996b)

	k_{ion}			k_{rec}			k_e		k_{ph}	
SPECIES	This work	Salama	Allain	This work	Salama	Allain	This work	Salama	This work	Salama
C_{16}	4.0E−9	4.0E−9	3.8E−9	6.0E−9	1.3E−8	3E−8	2.8E−9	5.3E−12	3.2E−8	4.0E−9
C_{24}	6.9E−9	5.8E−9	7.5E−9	6.0E−9	1.3E−8	3.5E−8	3.8E−9	7.2E−12	4.8E−8	4.8E−9
C_{32}	1.0E−8	...	8.4E−9	6.0E−9	...	4E−8		...		...
C_{50}	2.0E−8	...	9.8E−9	6.0E−9	...	5E−8	6.6E−9	...	1.0E−7	...
C_{100}	5.0E−8	1.7E−8	...	6.0E−9	4.4E−7	7E−8	1.1E−8	2.1E−8	2.0E−7	4.3E−8

Draine. Instead Salama et al. adopted an average UV field G_0 in units of Habing (1968) and an ionization cross section of about 2×10^{-18} cm^2 N_C^{-1} scaled to the number of carbon atoms, N_C, contained in the PAH.

For PAH cations we use the same UV absorption cross section as for neutrals, scaled to the total number of carbon atoms. However, an experiment on UV absorption of various PAHs, including pyrene and coronene, carried out by Robinson and collaborators (Robinson, Beegle, & Wdowiak 1997) suggests that PAH cations have a low UV absorption cross section below 7.75 eV. This corresponds mainly to the $\pi \rightarrow \pi^*$ transitions, which occur in the 3–8 eV range (see Fig. 11 in Paper I). It is thus important to check the effect of lowering the UV absorption cross section of cations in our model. To assess this question we have run our model for the three PAHs pyrene, coronene, and ovalene, assuming a UV absorption cross section for cations that includes only $\sigma \rightarrow \sigma^*$ and $\pi \rightarrow \sigma^*$ transitions (the rising curve above 8 eV in Fig. 11, Paper I). The effect of neglecting the transitions below 7.75 eV was found to be very small. This arises from the fact that high-energy photons around 10 eV or more, even if present at low levels in the normal interstellar UV field, are much more effective in the process of photodissociation; thus, the use of the same UV absorption cross section for neutrals and cations is justified.

Electron recombination rates.—The recombination rates reported by different workers show greater variations than the photoionization rates, reflecting the lack of experimental knowledge of the recombination of PAH^+ with electrons. Therefore, we must decide how to treat recombination rates in our model calculations. We start by assuming that the rate of recombination of PAH^+ species does not depend on size, and that only temperature effects are important. We therefore set the recombination rate for all species equal to the experimental value for the benzene cation, 1.0×10^{-6} cm^3 s^{-1} at 300 K (Abouelaziz et al. 1993).

Thus, at 100 K, assuming that the temperature dependence of the rate has the form $T^{-1/2}$, a total hydrogen density n_t of 25 cm^{-3}, and a ratio of electron density to total density n_e/n_t of 1.4×10^{-4}, the recombination rate will have the value $k_{\rm rec} = 1.0 \times 10^{-6}(300/100)^{1/2}(25)1.4 \times 10^{-4} = 6.0 \times 10^{-9}$ s^{-1}.

This expression for the recombination rate compares well with the values of Salama et al. (1996) for small PAHs. The factor of 2 difference arises from a n_e/n_t ratio of 3×10^{-4} in their work, as opposed to our adopted value of 1.4×10^{-4} (similarly, Allain et al. use $n_e/n_t = 4.4 \times 10^{-4}$).

However, for larger PAH^+ the rates diverge by almost 2 orders of magnitude. This is a consequence of using the theory of recombination of grains (Draine & Sutin 1987; Spitzer 1978), which assumes that the recombination is proportional to the size of the grain and that Coulomb focusing enhances the rate coefficient. In our calculation, Coulomb focusing is already included, as the rate is deduced from experimental work. Thus, the difference largely arises from the neglect of a size effect in our calculation. Our rates are also lower than those calculated by Allain et al. (1996a, 1996b), who used the theory of Spitzer (1978), applied to the recombination of grains but scaled through a sticking probability for electrons, so that their calculated rate agrees with the experimental recombination rate of benzene cation.

We can comment on the variation of the recombination rate coefficient with size. First, there is no experimental evidence for size dependence of the recombination rate; indeed the only rates which are known for PAH^+ species (for benzene and naphthalene cations) do not scale with size. These rates have been measured to be 1.0×10^{-6} and 3×10^{-7} cm^3 s^{-1} at 300 K, respectively (Abouelaziz et al. 1993). Second, it was recently found (Rebrion-Rowe et al. 2000) that substitution of a hydrogen atom in the benzene ring by another group such as methyl does not lead to an increase of the rate coefficient (as one might expect for a simple size-dependence law for the rate). Thus, there is no evidence for size dependence, at least for small PAH^+.

In our model we have chosen the recombination rate between the naphthalene cation and electrons as a standard value close to the common recombination rates, which have been measured for small polyatomic molecules ($\sim 3 \times 10^{-7}$ cm^3 s^{-1} at 300 K). Figure 5 displays the distribution of ovalene at different total hydrogen densities when a recombination rate equal to that of the benzene cation is assumed (10^{-6} cm^3 s^{-1} at 300 K). This figure is to be compared to Figure 1*c*, where the naphthalene rate is chosen, with other parameters being equal in both cases. The effect of such a variation in the recombination rate is not drastic and, apart from the different distribution between the neutral and cationic states, which is a direct consequence of the chosen value for the recombination rate, it can be seen that the generic shape of the distribution curves compare well with each other.

Electron attachment.—For the electron attachment rate, our work compares well with that of Salama et al. (1996), if we take into account the small sticking coefficient S of 10^{-3} that they used for small compact PAHs. In both caases it is assumed that the electron attaches to the PAH at the Langevin rate (Allamandola et al. 1989; Omont 1986):

$$k_{\rm L} = 2\pi e(\alpha/m_e)^{1/2} ,$$

where e and m_e are the electron charge and mass, and α is the polarizability of the neutral PAH. The remaining factor of 2 between our calculation and those of Salama et al. for PAHs bearing 100 carbon atoms and where the sticking coefficient is unity arises from the difference in the n_e/n_t ratio; note that the total rate in the table has the form

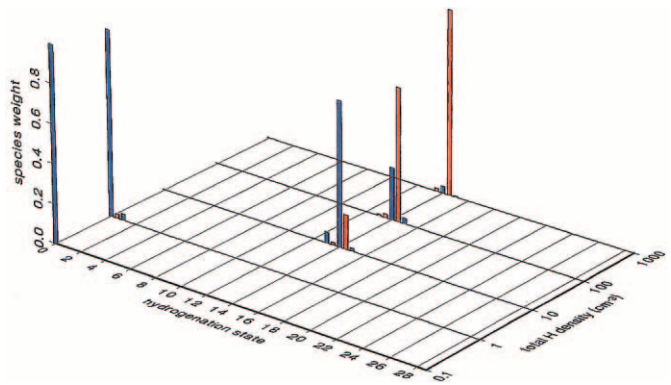

FIG. 5.—Distribution of a PAH bearing 32 carbon atoms in a standard environment where the total hydrogen density is varied, as in Fig. 1*c*, but with an alternate choice of the recombination rate with electrons. The chosen rate is the value measured for the benzene cation, while in Fig. 1*c* the recombination rate of naphthalene was chosen. For both figures a temperature of 100 K and a $T^{-1/2}$ temperature dependence were assumed. Blue bars represent cations and red bars represent neutrals.

$k_e = Sk_L n_e$ in units of s^{-1} and that the electron density is included.

Photodetachment.—For the photodetachment rate there is about 1 order of magnitude difference between our rate and that calculated by Salama et al. (1996). This difference may arise from the fact, as discussed in Paper I, that we use a tenfold larger number of photons that can photodetach the electron because we include photons over a wider energy range. Salama et al. include photons only in the 6–13.6 eV range, while we include all photons above 3 eV. As the interstellar field intensity is expected to show a steep increase for photons having an energy below 5 eV (see Fig. 3 in Paper I), and because the electron affinities of PAH are expected to be lower than 3 eV, it is likely that these photons represent a major contribution to photodetachment.

Remarks on the rates for ionization processes.—This short discussion on the main processes that control the ionization balance of PAHs in the diffuse ISM shows that, apart from ionization, which seems to be known with sufficient accuracy, the numerical values of other rates are still open to speculation. Thus, an accurate determination of these rates will only be possible when more experimental data become available. In this respect, a study of the recombination rate for a large PAH such as coronene will be very valuable, and will be helpful in investigating more accurately the dependence of the electron recombination rate on size. Moreover, the lack of photodetachment cross sections for PAH^- makes the calculation of the proportion of PAH anions in the ISM somewhat speculative.

4. SUMMARY OF RESULTS

4.1. *Hydrogenation in Low- to Moderate-Density Clouds*

For diffuse clouds in which densities are too low to support a large anion population (i.e., $n_t < 100$ cm^{-3}), we can separate PAHs into four categories according to size: very small PAHs (fewer than about 15–20 carbon atoms) are destroyed in the ISM; small PAHs (from 20 to about 30 carbon atoms) are extremely dehydrogenated; PAHs in the 30–40 carbon range, which are hydrogenated but prone to C_2H_2 loss (see end of § 4); and finally, PAHs with more than 40 carbon atoms, which can survive in the ISM with their normal hydrogen coverage.

This analysis leads to the interesting possibility that PAHs are split into two distinct populations: one consisting of highly dehydrogenated PAHs having carbon numbers in the 20–30 range, and a second population containing fully hydrogenated PAHs bearing more than 30 carbon atoms. PAHs having fewer than 20 carbon atoms would not survive because of photodissociation. These size ranges depend primarily on the photodissociation rate rather than the hydrogenation rate, because photodissociation is very size-dependent, while the hydrogenation rate is much less so.

4.2. *Hydrogenation in Dense Clouds: The Role of PAH Anions*

We have neglected the possible contribution of anion chemistry in our model; however, this neglect is not justified in dense environments. For example, in an extreme scenario, for small species like pyrene or coronene in an environment of high hydrogen density (around 100 cm^{-3} or higher), the neglect of anions is not justified (Fig. 4). This effect is exacerbated by the expected decrease of the UV field intensity through enhanced dust extinction, which will further decrease the proportion of cations.

As an example, coronene molecules immersed in a cloud where $n_t = 100$ cm^{-3} and $\chi = 0.5$ will be distributed among their three charge states as follows: the anions representing about 20%, the neutrals 70%, and the cations only 10%. For such conditions the neglect of the anion chemistry is no longer valid. If we assume that the anions have reactivities with hydrogen atoms similar to those of the cations, the neglect of anions could lead (for high-density clouds) to an underestimate of the hydrogenation rate by a factor of 3 (for anion densities equaling twice the cation contribution).

The overall effect of this neglect would be a lowering of the PAH size for which the hydrogenation rate would balance the photodissociation rate; if we take into account the anion chemistry, the equilibrium will be reached for a species for which the photodissociation rate can be 3 times larger, thus lowering the PAH size for which the balance is accomplished. However, around the size of coronene or ovalene, where this equilibrium is expected to occur, the photodissociation rate of PAHs becomes a strong function of the PAH size, and thus an enhancement of the photodissociation rate by a factor of 3 corresponds to a lowering of the PAH size by only 2 or 3 carbon atoms. Thus, the neglect of anion chemistry, even in the high-density cases in which anions dominate over cations, will have only a small effect on the PAH size where the hydrogenation rate is balanced by the photodissociation rate. This seemingly paradoxical result is to be expected if one recalls that the most rapidly varying rate is likely to control the equilibrium.

This discussion shows that the three different divisions of PAHs (too small to survive, extremely dehydrogenated, and normally hydrogenated) are mainly dependent on the calculation of the photodissociation rate rather than the precise estimation of the hydrogenation rates.

4.3. *Size-Dependent Behavior*

In this section we combine all of the processes considered in our simple two-frequency RRKM theory (see Paper I) to estimate the rates that lead to C_n loss, H loss, or C_2H_2 loss, and thus arrive at final estimates of the relative importance of different states of hydrogenation and ionization. As discussed previously, the rate coefficient for each process will depend on three parameters: the molecular size, the threshold energy associated with the process, and the $\Delta S^{\neq}_{1000\,\mathrm{K}}$ parameter, which we introduced in Paper I. For this latter parameter we used an entropy change of about 5 cal K^{-1} for processes for which no data are available.

The loss of a C_n fragment after UV absorption has been estimated by Léger et al. (1989) to be endothermic by about 8 eV. We have performed a semiempirical calculation of the process $C_{16}^+ \rightarrow C_{14}^+ + C_2$ using the MOPAC 6.0 program (Stewart 1988) and found that this process requires about 10 eV, in rough agreement with the estimate of Léger et al. The carbon skeleton of the pyrene structure was assigned to the C_{16}^+ ion, while the phenanthrene structure was chosen for C_{14}^+. We also used the GAUSSIAN 94 program (Frisch et al. 1995) and found the same estimation at the ROMP2/6-31g*//ROHF/6-31g* level of calculation. This result is consistent with a C_2 loss where two bonds are broken. We thus adopt a value of 8 eV for C_n loss, in agreement with the estimate of Léger et al. as well as Omont (1986), who have proposed a value of 8.5 eV.

For the H loss threshold we employ a value of 4.8 eV, which is close to the dissociation energy of a CH bond in a neutral PAH. This value is also similar to the CH bond energy in large PAH cations. The $\Delta S^{\neq}_{1000\,\mathrm{K}}$ is estimated to be about 5 cal K^{-1}, in agreement with the experimental values given in Paper I.

The C_2H_2 loss process for small PAHs requires about 4.5 eV, based on an estimate of the experimental values for benzene, naphthalene, phenanthrene, and anthracene cations. When a C_2H_2 fragment is ejected from a PAH it is likely that the required energy is close to the value of two single C—C bonds minus the energy difference between a double C=C and a triple C≡C bond (neglecting any resonance energy). This value is estimated to be approximately equal to $2 \times 80 - (195 - 140) = 105$ kcal mol^{-1} ($= 4.55$ eV); $\Delta S^{\neq}_{1000\,\mathrm{K}}$ is estimated to be about 10 cal K^{-1}, in agreement with the experimental values, which are in the range of 8–12 cal K^{-1} for these species (Ling et al. 1998; Gotkis et al. 1993b).

However, large PAHs preferentially lose an H atom rather than a C_2H_2 fragment, and thus it is likely that the activation energy for acetylenic loss is greater than 4.8 eV, which corresponds to the activation energy expected for H loss in large PAHs. For example, in the study of Jochims et al. (1994) on pyrene cation, the appearance potential for H loss and C_2H_2 loss were found to be 9.06 and 10.35 eV, respectively, leading to the conclusion that H loss is favored over C_2H_2 loss for this cation. In their experimental setup the excited ions were detected 10^{-4} s after photoexcitation. Thus, the appearance potentials reported by Jochims et al. are the internal energies of ions corresponding to a photodissociation rate of $10^4\ \mathrm{s}^{-1}$.

With our RRKM procedure, and assuming $\Delta S^{\neq}_{1000\,\mathrm{K}}$ values of 5 and 10 cal K^{-1}, respectively, for H loss and for C_2H_2 loss, we have varied the activation energies of both processes so that our calculation would reproduce the results of Jochims et al. This was achieved for a difference of 0.7 eV between the activation energies for C_2H_2 loss and H loss, and thus we might assume that the endothermicity of the acetylenic loss process is 5.5 eV in the case of the pyrene cation. Moreover, for the coronene cation, which is the larger PAH in their study, the C_2H_2 loss fragmentation channel was not detected while the H loss channel was observed. Thus, it is probable that the C_2H_2 loss process for larger PAHs such as coronene or ovalene requires even more than 5.5 eV, and consequently, we tentatively assign a value of 6.0 eV for this activation energy for large PAH cations.

Finally, there is another process that could further divide PAHs into two different groups in the case of very large PAHs: the loss of hydrogen atoms bound to a carbon atom bearing two H atoms. We have discussed this process of extra hydrogenation of PAH^+ in Paper I as a possible mechanism which can lead to more extensively hydrogenated PAHs, with peripheral carbon atoms being aliphatic (e.g., benzene converted to cyclohexane). If we compare the heat of formation of benzene to that of cyclohexane, we deduce an average CH bond energy of about 2.6 eV (Lias et al. 1988). However, the ab initio calculation of Mebel et al. (1997) gives, for the process $C_6H_7 \rightarrow C_6H_6 + H$, an activation energy of about 1.2 eV. This low activation energy is probably due to the radical character of C_6H_7, as well as the aromaticity of C_6H_6, which may facilitate the reaction. Thus, it is likely that the average energy needed to eject an H atom bound to an aliphatic carbon is somewhere between these two values of 1.2 and 2.6 eV. Consequently, we assign an activation energy of 2 eV for this process. The corresponding $\Delta S^{\neq}_{1000\,\mathrm{K}}$ parameter was chosen to be equal to 0.0 cal K^{-1}, in agreement with the ab initio calculation of Mebel et al. The results of the calculations are shown in Figures 6 and 7.

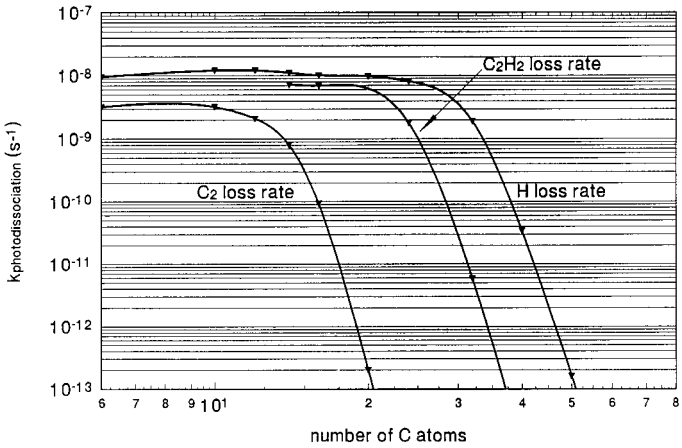

FIG. 6.—Photodissociation rates of extremely dehydrogenated PAHs with ejection of a C_2, C_2H_2, or H fragment. The C_2 loss rate is greater than the C^+ insertion on neutral PAHs for PAHs with fewer than about 18 carbon atoms; thus, these small PAHs are quickly destroyed in the ISM unless there is an efficient mechanism that creates these PAHs. PAHs with fewer than about 30 carbon atoms are mostly dehydrogenated because the rate of H loss is greater than the rate of radiative H addition. Note that these limits are calculated for PAHs immersed in a cloud where $\chi = 1$ and $n_t = 25\ \mathrm{cm}^{-3}$. PAHs in the 20–30 carbon atom range are thus extremely dehydrogenated, but their carbon skeletons are possibly able to withstand the strong UV photons without undergoing fragmentation. These PAH can grow through carbon insertion, but when they approach the 30 carbon size they become partially hydrogenated, and thus they are prone to C_2H_2 loss. The overall effect may be a stabilization of these small dehydrogenated PAHs somewhere in the range of 20–30 carbon atoms.

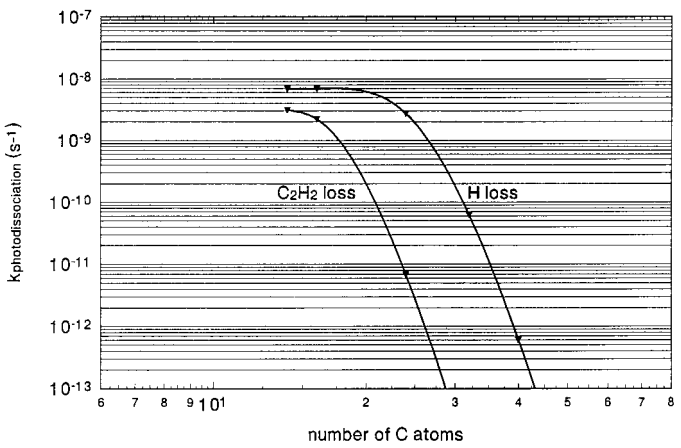

FIG. 7.—Rates of photodissociation for PAHs having their normal hydrogen coverage. The calculations were made on the following PAHs: $C_{14}H_{10}$, $C_{16}H_{10}$, $C_{24}H_{12}$, $C_{32}H_{14}$, and $C_{50}H_{20}$. Normally hydrogenated coronene maintains its hydrogen coverage in a normal interstellar UV field. In this calculation it is also assumed that $n_t = 25\ \mathrm{cm}^{-3}$ and $\chi = 1$, as in Fig. 5. This explains why for coronene and ovalene the hydrogenation state distribution is sometimes split into an extremely dehydrogenated distribution and a normally hydrogenated distribution (see Figs. 1*b* and 3*b*, for example).

Figure 6 compares the rate of H loss with the rate of hydrogenation of PAH cations and the rate of C_2 and C_2H_2 losses with the rate of C^+ insertion on neutral PAHs. It is assumed that the hydrogen density is 25 cm^{-3} and that the rate of H addition is about 10^{-10} cm^3 s^{-1}, thus leading to a first-order rate of 2.5×10^{-9} s^{-1}.

Reactions between C^+ and neutral PAHs are assumed to proceed near the collision rate, with a rate coefficient of 10^{-9} cm^3 s^{-1}. This process has been suggested by Thaddeus (1995) as a mechanism that allows carbon chains to grow in the ISM. Furthermore, in their study of the distribution of PAHs in the Galaxy, Giard et al. (1994) have suggested that there is a direct formation mechanism for PAHs in the ISM; C^+ insertion could participate in this process. Canosa et al. (1995) have experimentally detected C^+ insertion on neutral anthracene. Thus, in our model the rate of insertion is equal to the density of C^+ times the collision rate, leading to a value of about 3.5×10^{-12} s^{-1}. In Figure 6, PAHs are extremely dehydrogenated, while in Figure 7 they bear their normal hydrogen coverage; thus, in the latter figure it is implicitly assumed that the rate of H loss is lower than the hydrogenation rate.

From Figure 6 a minimum size for the stability of the carbon skeleton can be calculated to be about 18–20 carbon atoms. It is also clear that PAHs with 20–30 carbon atoms will be almost completely dehydrogenated because the H loss rate is larger than the H addition rate in this range. After a few C^+ insertions on a small, extremely dehydrogenated PAH (when this species is neutral) with about initially 20 carbon atoms, it is possible that the increased number of degrees of freedom allows subsequent additions of H atoms (when the species is cationic). However, it is likely that as the PAH^+ adds hydrogen atoms it will also lose C_2H_2. Thus, it is possible that the molecule will not escape this size window of 20–30 carbon atoms, because acetylenic loss will prevent the PAH from growing larger.

If this mechanism is efficient, this may be an answer to the criticism of the PAH hypothesis that argues that PAHs will grow by C^+ insertion at an unacceptably high rate (Thaddeus 1995), thus depleting the C^+ reservoir in a very short time. If the C_2H_2 loss mechanism were not efficient, we could roughly estimate the survival time of the C^+ reservoir to be equal to the time needed for neutral PAH to consume the carbon cations through C^+ insertion. If we assume that 10% of the total carbon is locked into PAHs having a size of about 30 carbons, and if we choose the Langevin rate k_L for the accretion rate, then the lifetime of the C^+ reservoir would be $\tau_{C^+} = (k_L \times n_{PAH})^{-1}$ where n_{PAH} is the total PAH density, which is about $2.25 \times 10^{-4}(0.1/30)n_t$ under our assumptions, and with a total carbon density of 225 p.p.m. (Snow & Witt 1995). If we assume the total hydrogen density n_t to be 100 cm^{-3}, and if the polarizability α of neutral PAHs is $0.9(N_C)^{3/2}$ (see Paper I), this will lead to a lifetime τ_{C^+} of about 5×10^4 yr; this is much lower than the typical lifetime of a diffuse cloud. If we assume that the polarizability of the PAHs scale with the total number of carbon atoms of the PAH according to the formula given by Allamandola et al. (1989), $\alpha = 1.5N_C$, then the lifetime would be about 1×10^5 yr. However, this still appears to be smaller than the typical lifetime of a diffuse cloud, which is expected to be about 10^6 yr (Wagenblast 1992). This suggests that PAHs, if present in the diffuse ISM, are mostly concentrated in the size range in which the C_2H_2 loss process efficiently returns the accreted C^+ to the C^+ reservoir. Thus, assuming that condensation reactions are negligible, it is probable that the larger PAHs containing 50 carbon atoms or more are in lower concentration than the smaller PAHs, which are prone to acetylene loss, because for the large PAHs there are probably no mechanisms that oppose the rapid accretion of the C^+ species.

These results suggest that small, extremely dehydrogenated PAHs, with about 20–30 carbon atoms, are possible candidates as DIB carriers. Moreover, the limited number of PAH isomers in this size range provides a solution to the "isomer explosion" problem. This term refers to the very large number of possible different PAH isomers and the difficulty of finding a selection mechanism that allows only a small number to persist in the ISM, in agreement with the limited number of DIBs. Moreover, the C_2H_2 loss process will tend to homogenize and stabilize the PAHs in a narrow size range.

However, the above limit of 30 carbon atoms should also be examined for the case of normally hydrogenated PAHs, because PAHs with more than 30 carbon atoms should bear a normal hydrogen coverage. This is done in Figure 7, where the loss of hydrogen and C_2H_2 are compared to the corresponding addition rates with H and C^+ (addition between neutral PAHs and C^+ is assumed to proceed at the Langevin rate; see the experimental work of Canosa et al. [1995] for the reaction between C^+ and anthracene; the addition reaction between coronene and C^+ is also fast [E. Keheyan 2002, private communication]). It is assumed that for compact PAHs there are six different possibilities for C_2H_2 loss, and thus the photodissociation rate is multiplied by a factor of 6. However, the overall effect is a lowering of the limit of the rate of C_2H_2 loss, because the additional hydrogen atoms attached to the carbon skeleton strongly stabilize the molecule. The same effect of stabilization of the PAH also holds in the case of H loss, and this figure indicates that a coronene molecule is able to withstand the UV field without extensive loss of H atoms. Similarly, Figures 3*b* and 1*b* show that both forms of PAH are important and that stability is achieved for both the dehydrogenated and hydrogenated PAHs.

Finally, for very large PAHs, with about 150–200 carbon atoms, the rate of hydrogenation of the PAHs is equal to the rate of H loss from aliphatic carbon atoms. Thus, it may happen that PAHs containing more than 200 carbon atoms are highly hydrogenated in the ISM. However, the size limit at which this occurs strongly depends on the endothermicity assumed for the process $PAHH \rightarrow PAH + H$, and as this endothermicity is still poorly known, it is possible that the size for which PAHs become extensively hydrogenated is much larger (see Fig. 8).

5. ASTROPHYSICAL IMPLICATIONS AND FURTHER WORK

If we assume that PAHs are present in the diffuse interstellar medium and that they may consume 1%–10% of the carbon budget, then it is rather certain that such molecules, with a collective density as high as 10^{-7} to $10^{-6}n_t$, will have profound implications on the cloud behavior. In this last section we briefly investigate the major reactions that PAHs can undergo in the presence of other cloud constituents. All reactions with these minor species occur within a timescale longer than a few hundred years, and thus it can be assumed that the PAH distribution prior to reaction is the one

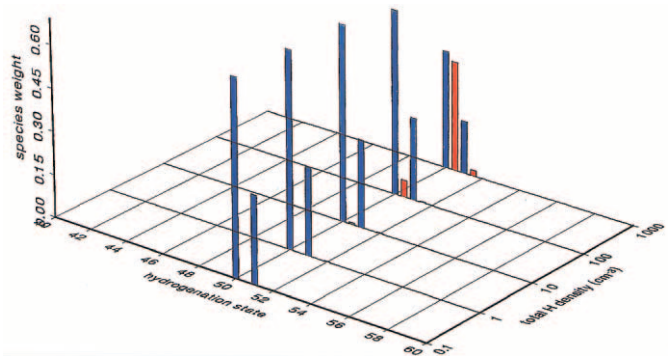

FIG. 8*a*

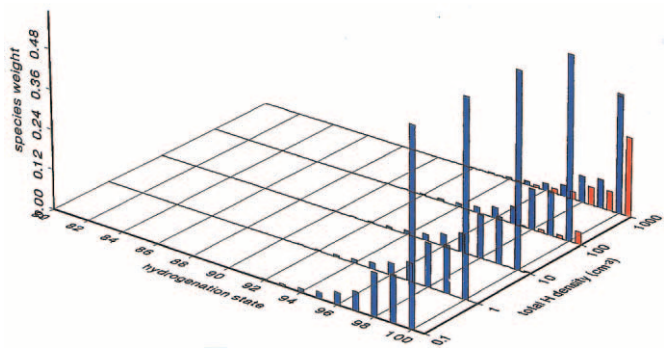

FIG. 8*b*

FIG. 8.—Hydrogenation and charge distribution of a PAH bearing 200 carbon atoms, illustrating the importance of the endothermicity of the dissociative channel $PAHH + h\nu \rightarrow PAH + H$. Blue bars represent cations and red bars represent neutrals. In (*a*) an endothermicity of 1.16 eV was chosen, in agreement with the calculation of Mebel et al. (1997) on the benzene system. As this calculation may be only representative of the benzene system, an alternate value of 2.0 eV was chosen for (*b*), leading to the complete hydrogenation of the C_{200} species. The effect of this change in endothermicity is drastic, and thus it is not possible to estimate at what size the PAH can be expected to be fully hydrogenated. However, the complete hydrogenation of PAH can take place probably only for PAHs with more than 100 carbon atoms.

calculated using the frame presented in Paper I. Among the most important reactions we need to consider are the reactions between the PAH bearing about 30 carbon atoms, possibly ionized, and C^+, O, and N, as well as reactions between PAH cations and PAH neutrals.

For this latter reaction we can derive a typical lifetime τ_{PAH} equal to $(n_{PAH} \times k_L)^{-1}$, where the Langevin rate k_L is now calculated using a reduced mass $\mu = 15m_C$, where m_C is the carbon atom mass. If we assume $n_t = 100$ cm^{-3} and that the collective density of PAH is about $3.75 \times 10^{-7} n_t$ (i.e., $0.5 \times 2.25 \times 10^{-4} n_t$ (0.1/30), the factor 0.5 coming from the expected fraction of neutral PAH, see Paper I), then the lifetime τ_{PAH} will be equal to about 0.7 Myr, in rough agreement with an expected lifetime of about 1 Myr for the cloud. This process will possibly convert small dehydrogenated PAHs in the 20–30 carbon atom range to larger PAHs containing about 40–60 carbon atoms and thus with enough degrees of freedom to allow a complete hydrogenation of the carbon skeleton. For these large PAHs the protonated form $PAHH^+$ might efficiently compete with the normal PAH^+ species. In our model, electron recombination of these $PAHH^+$ are still dissociative processes because of the small expected endothermicity of the $PAHH \rightarrow PAH_{-1} + H_2$ reaction; this might prove to be an alternative initial H_2 formation process in diffuse clouds where the temperature and high UV flux may prevent grains from efficiently producing molecular hydrogen.

Reaction between PAH^+ and O atoms lead to the probable formation of epoxy structures (Le Page et al. 1999a). The lifetime of dehydrogenated PAH cations with respect to O addition can be estimated to be about $(k_O \times n_O)^{-1}$, where k_O is the rate of addition of O atoms, which is expected to be equal to about 10^{-10} cm^3 s^{-1} (Snow et al. 1998), and n_O is the oxygen density, which we choose to be $3.2 \times 10^{-4} n_t$ (Meyer, Jura, & Cardelli 1998). If we assume $n_t = 100$ cm^{-3} this leads to a lifetime of only 10^4 yr for PAH^+ against O addition, which is far smaller than the expected lifetime for PAH of about 1 Myr as estimated above. However, it is probable that the O atom will not stick for a very long time to the PAH^+ carbon skeleton, because the binding energy is rather small. Indeed, an estimation using the MOPAC 6.0 semiempirical program (Stewart 1988) leads to only about 3 eV for the binding energy between an O atom and the dehydrogenated pyrene cation C_{16}^+. Thus, even if O atoms are able to associate to small dehydrogenated PAH cations, it is expected that the available UV photons will quickly remove them from the carbon skeleton within a year (assuming $E_0 = 3.3$ eV and $\Delta S^{\neq}_{1000\,K} = 0.0$ eu, the photodissociation process $C_{30}O^+ + h\nu \rightarrow C_{30}^+ + O$ is found to have a typical time of about 1.4 yr only when using our 2ν RRKM model presented in Paper I). For $PAHs^+$ that result from PAH coalescence (e.g., $C_{30}^+ + C_{30} \rightarrow C_{60}^+$, with subsequent hydrogenation), however, the addition of O atoms could be more efficient, as the number of degrees of freedom is much larger, and thus these large PAHs might bear few oxygen atoms. Further association of these PAHs might lead to amorphous carbonaceous macromolecules similar to those proposed by Papoular (2000), in which PAHs are bonded together using O bridges.

It has been found that the reaction between O and small PAH^+ can produce CO, and this can be another depletion mechanism for PAH cations (Snow et al. 1998; Le Page et al. 1999b). However, the branching ratio of the channel $PAH^+ + O \rightarrow (PAH - C)^+ + CO$ was found to drastically decrease in favor of the association product $PAHO^+$ as the PAH size increases (from 1 and 0.55 for the benzene and naphthalene cations, respectively, to less than 0.05 for the pyrene cation at helium densities of about 10^{16} cm^{-3}). Thus, the C^+ insertion on neutral PAH, if proceeding at the Langevin rate, is a few orders of magnitude larger than the expected loss of C on PAH cations through CO production, and thus the overall balance favors the addition of carbon atoms. However, in order to estimate the precise rate of CO formation the branching ratio should be estimated at the low densities prevailing in the ISM.

The reactions between N atoms and PAH cations, which can produce HCN (Le Page et al. 1999b), are probably of less importance than the reactions involving O atoms, because it has been found that most reactions between N atoms and PAH^+ are slow due to spin conservation.

The C_2H_2 loss process might not be the only mechanism which prevents small dehydrogenated PAH cations from growing larger. The binding energy between a C atom and a dehydrogenated PAH seems to be much larger than the one for O addition (about 8 and 5 eV in the cation and neutral cases, respectively, as estimated from semiempirical calculations on the dehydrogenated pyrene species). Thus, the removal of C atoms from the PAH skeleton is a difficult

process which may require over 10^3 yr in the standard UV interstellar field. Accordingly, it may happen that the PAH cation becomes doubly ionized during this period because the typical times for sequential double ionization are about 10^3 yr for many PAHs (see Paper I), as estimated from the corresponding ionization potentials measured by Tobita et al. (1994). Such a PAH^{++} with a single carbon attached to the skeleton might react dissociatively with the abundant H atoms to form a CH^+ fragment with a high kinetic energy of about 1 eV or even more due to electrostatic repulsion between the two fragments. Or, alternatively, if the reaction with H is not dissociative in this first step, the subsequent absorption of a UV photon can lead to the same product through photodissociation. The ejected CH^+ species will probably not react very efficiently with H atoms to form $C^+ + H_2$, because this reaction rate was found to drastically decrease with increasing energy of the CH^+ ion (Federer et al. 1985); thus, the CH^+ ions will remain in the ISM for a few years before either recombining dissociatively with electrons, or reacting with H or H_2 after partial relaxation of its kinetic energy. This mechanism could significantly contribute to the production of CH^+ in diffuse clouds, possibly competing with other mechanisms of formation of this ion, like the $C^+ + H2$ reaction in vorticity (Falgarone et al. 1995). Moreover, the efficiency of CH^+ formation catalysed by PAH is enhanced because the CH^+ ion may survive longer due to its kinetic energy and because it involves a fast reaction between an ion and a neutral PAH with high polarizability.

Finally, it is worth noting that a bimodal distribution of PAHs, such as the one proposed in this paper, where the whole population of PAHs is split into small dehydrogenated PAHs and larger PAHs in their normal hydrogenation state, strongly supports independent recent work from Duley & Seahra (1999a, 1999b). This study shows that the 2175 Å peak and the extended red emission near 700 Å can be reproduced using a superposition of a central peak arising from dehydrogenated coronene and a somewhat broader peak due to larger hydrocarbons with $N_C > 64$. Our model not only agrees with this proposal but also presents a physical basis for the occurrence of such a bimodal distribution (see Fig. 9).

All the above processes which are possible signatures of PAHs in the diffuse medium deserve a careful analysis and will be the subject of a forthcoming paper. Another important point is the inclusion of a realistic dust model in our work, as well as the implementation of the chemistry outlined in this last section. This will allow coupling of all the hydrogenation distributions calculated in this paper and an estimation of their relative proportions.

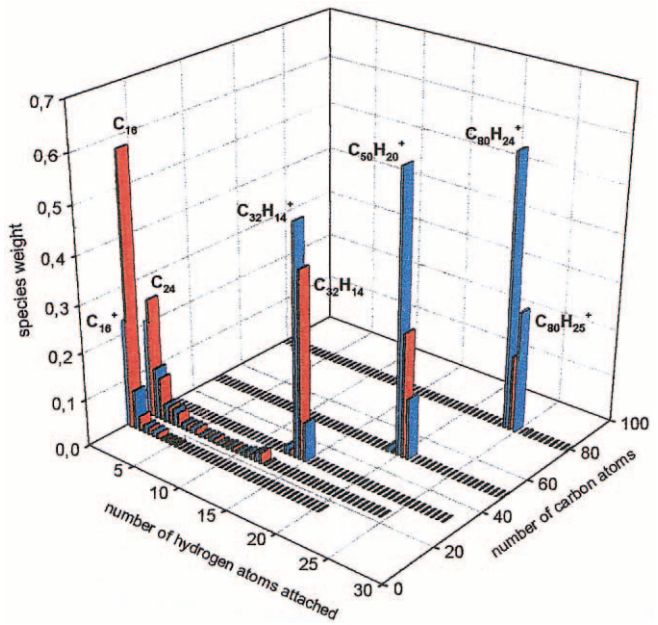

FIG. 9.—Distribution of the charge and hydrogenation states of five different PAHs families ($C_{16}H_n$, $C_{24}H_n$, $C_{32}H_n$, $C_{50}H_n$, and $C_{80}H_n$) in a diffuse cloud where the environmental parameters are set to $n_t = 100$ cm^{-3}, $f = 0.5$, $\chi = 1$, $T = 100$ K, and $n_e/n_t = 1.4 \times 10^{-4}$. Red bars represent neutrals and blue bars represent cations. The $C_{16}H_n$ and $C_{24}H_n$ families are concentrated in the lowest hydrogenation states, while the $C_{32}H_n$, $C_{50}H_n$, and $C_{80}H_n$ families have a distribution peaked at their normal hydrogenation states (i.e., $C_{32}H_{14}$, $C_{50}H_{20}$, and $C_{80}H_{24}$). For larger families the protonated form (e.g., $C_{80}H_{25}^+$) is present at an appreciable level.

6. CONCLUSIONS

PAHs in the diffuse ISM may undergo a variety of hydrogenation and dissociation processes. We classify PAHs into four different groups, with limits depending on the size of the molecule and the local environment:

1. Very small PAHs with sizes smaller than about 15–20 carbon atoms. These PAHs are quickly destroyed in the normal UV field and thus returned to the C^+ reservoir after subsequent multiple photodissociation reactions.
2. Small PAHs which contain between 20 and 30 carbon atoms. These PAHs are extremely dehydrogenated and may grow via carbon insertion on the neutral and subsequently by addition of hydrogen. However, these species are then prone to C_2H_2 loss, a process that may maintain the PAH size below a limit of about 30 C, *assuming that condensation reactions are negligible*.
3. Large PAHs with more than 30 carbon atoms. These PAHs have normal hydrogen coverage with competition from the protonated form.
4. Very large PAHs. These species can be more highly hydrogenated with some of the peripheral carbon atoms bearing two H atoms.

Finally, it has been shown that photodissociation is the most critical process governing the PAH behavior in the diffuse ISM.

We gratefully acknowledge support of this work by NASA.

REFERENCES

Abouelaziz, H., Gomet, J. C., Pasquerault, D., Rowe, B. R., & Mitchell, J. B. A. 1993, J. Chem. Phys., 99, 237
Allain, T., Leach, S., & Sedlmayr, E. 1996a, A&A, 305, 602
———. 1996b, A&A, 305, 616
Allain, T., Sedlmayr, E., & Leach, S. 1997, A&A, 323, 163
Allamandola, L. J., Tielens, A. G. G. M., & Barker, J. R. 1989, ApJS, 71, 733
Bakes, E. L. O., & Tielens, A. G. G. M. 1994, ApJ, 427, 822
Barker, J. R. 1983, Chem. Phys., 77, 301
Bates, D. R. 1988, in Molecular Astrophysics, ed. T. W. Hartquist (Cambridge: Cambridge Univ. Press), 211
Benson, S. W. 1976, Thermochemical Kinetics (New York: Wiley Interscience)
Bernstein, M. P., Sandford, S. A., & Allamandola, L. J. 1996, ApJ, 472, L127

Bohme, D. K. 1992, Chem. Rev., 92, 1487
Canosa, A., Laubé, S., Rebrion, C., Pasquerault, D., Gomet, J. C., & Rowe, B. R. 1995, Chem. Phys. Lett., 245, 407
Crawford, M. K., Tielens, A. G. G. M., & Allamandola, L. J. 1985, ApJ, 293, L45
Dartois, E., & d'Hendecourt, L. 1997, A&A, 323, 534
Draine, B. T., & Sutin, B. 1987, ApJ, 320, 803
Du, P., Salama, F., & Loew, G. H. 1993, Chem. Phys., 173, 421
Duley, W. W., & Seahra, S. S. 1999a, ApJ, 520, 719
———. 1999b, ApJ, 522, L129
Duley, W. W., & Williams, D. A. 1986, MNRAS, 219, 859
Falgarone, E., Pineau des Forêts, G., & Roueff, E. 1995, A&A, 300, 870
Federer, W., Villinger, H., Tosi, P., Bassi, D., Ferguson, E., & Lindinger, W. 1985, in Molecular Astrophysics, ed. G. H. F. Diercksen et al. (Dordrecht: Reidel), 649
Feng, W. Y., & Lifshitz, C. 1996, Int. J. Mass Spectrom. Ion Processes, 152, 157
Frenklach, M., & Feigelson, E. D. 1989, ApJ, 341, 372
Frisch, M. J., G. W., et al. 1995, Gaussian 94 (Revision C.2; Pittsburgh: Gaussian Inc.)
Giard, M., Lamarre, J. M., Pajot, E., & Serra, G. 1994, A&A, 286, 203
Giles, K., Adams, N. G., & Smith, D. 1989, Int. J. Mass Spectrom. Ion Processes, 89, 303
Gotkis, Y., Naor, M., Laskin, J., Faulk, J. D., & Dunbar, R. C. 1993a, J. Am. Chem. Soc., 115, 7402
Gotkis, Y., Oleinikova, M., Naor, M., & Lifshitz, C. 1993b, J. Phys. Chem., 97, 12282
Habing, H. J. 1968, Bull. Astron. Inst. Netherlands, 19, 421
Ho, Y.-P., Dunbar, R. C., & Lifshitz, C. 1995, J. Am. Chem. Soc., 117, 6504
Joblin, C. 1992, Ph.D. thesis, Univ. Paris VII
Jochims, H. W., Rasekh, H., Rühl, E., Baumgärtel, H., & Leach, S. 1993, J. Phys. Chem., 97, 1312
Jochims, H. W., Rühl, E., Baumgärtel, H., Tobita, S., & Leach, S. 1994, ApJ, 420, 307
Joulain, K., Falgarone, E., Pineau des Forêts, G., & Flower, D. 1998, A&A, 340, 241
Kaiser, R. I., Asvany, O., & Lee, Y. T. 2000, Planet. Space Sci., 48, 483
Klippenstein, S. J., Faulk, J. D., & Dunbar, R. C. 1993, J. Chem. Phys., 98, 243
Leach, S. 1987, in Polycyclic Aromatic Hydrocarbons and Astrophysics, ed. A. Léger, L. d'Hendecourt, & N. Boccara (Dordrecht: Reidel), 99
Léger, A., Boissel, P., Désert, F. X., & d'Hendecourt, L. 1989, A&A, 213, 351
Léger, A., & d'Hendecourt, L. 1985, A&A, 146, 81
Le Page, V., Keheyan, E., Bierbaum, V. M., & Snow, T. P. 1999a, J. Am. Chem. Soc., 121, 9435
Le Page, V., Keheyan, E., Snow, T. P., & Bierbaum, V. M. 1999b, Int. J. Mass Spectrom, 185, 949
Le Page, V., Snow, T. P., & Bierbaum, V. M. 2001, ApJS, 132, 233 (Paper I)
Lepp, S., & Dalgarno, A. 1988, ApJ, 324, 553
Lias, S. G., Bartmess, J. E., Liebman, J. F., Holmes, J. L., Levin, R. D., & Mallard, W. G. 1988, J. Phys. Chem. Ref. Data, 17, S1
Ling, Y., Gotkis, Y., & Lifshitz, C. 1995, European Mass Spectrom., 1, 41
Ling, Y., & Lifshitz, C. 1998, J. Phys. Chem. A, 102, 708
Ling, Y., Martin, M. L., & Lifshitz, C. 1997, Int. J Mass Spectrom. Ion Processes, 160, 39
Mebel, A. M., Lin, M. C., Yu, T., & Morokuma, K. 1997, J. Phys. Chem. A, 101, 3196
Meyer, D. M., Jura, M., & Cardelli, J. A. 1998, ApJ, 493, 222
Millar, T. J. 1992, MNRAS, 259, P35
Omont, A. 1986, A&A, 164, 159
Papoular, R. 2000, A&A, 362, L9
Pauzat, F., & Ellinger, Y. 2001, MNRAS, 324, 355
Petrie, S., Javahery, G., & Bohme, D. K. 1992, J. Am. Chem. Soc., 114, 9205
Rebrion-Rowe, C., Mostefaoui, T., Laubé, S., & Mitchell, J. B. A. 2000, J. Chem. Phys., 113, 3039
Robinson, M. S., Beegle, L. W., & Wdowiak, T. J. 1997, ApJ, 474, 474
Rühl, E., Price, S. D., & Leach, S. 1989, J. Phys. Chem., 93, 6312
Sablier, M., & Rolando, C. 1993, Mass Spectrom. Rev., 12, 285
Salama, F., Bakes, E. L. O., Allamandola, L. J., & Tielens, A. G. G. M. 1996, ApJ, 458, 621
Schutte, W. A., Tielens, A. G. G. M., & Allamandola, L. J. 1993, ApJ, 415, 397
Scott, G. B. I., Fairley, D. A., Freeman, C. G., McEwan, M. J., Adams, N. G., & Babcock, L. M. 1997, J. Phys. Chem. A, 101, 4973
Snow, T. P., Bakes, E. L. O., Buss, R. H., & Seab, C. G. 1995, A&A, 296, L37
Snow, T. P., Le Page, V., Keheyan, Y., & Bierbaum, V. M. 1998, Nature, 391, 259
Snow, T. P., & Witt, A. N. 1995, Science, 270, 1445
Sofia, U. J., Cardelli, J. A., Guerin, K. P., & Meyer, D. M. 1997, ApJ, 482, L105
Spitzer, L. 1978, Physical Processes in the Interstellar Medium (New York: Wiley Interscience)
Stewart, J. J. P. 1988, J. Comp. Chem., 10, 221
Tobita, S., Leach, S., Jochims, H. W., Rühl, E., Illenberger, E., & Baumgärtel, H. 1994, Canadian J. Phys., 72, 1060
Thaddeus, P. 1995, in The Diffuse Interstellar Bands, ed. A. G. G. M. Tielens & T. P. Snow (Dordrecht: Kluwer), 369
van der Zwet, G., & Allamandola, L. J. 1985, A&A, 146, 76
van Dishoeck, E. F., & Black, J. H. 1986, ApJS, 62, 109
Verstraete, L., Léger, A., d'Hendecourt, L., Dutuit, O., & Défourneau, D. 1990, A&A, 237, 436
Vuong, M. H., & Foing, B. H. 2000, A&A, 363, L5
Wagenblast, R. 1992, MNRAS, 259, 155